C. R. Acad. Sci. Paris, Ser. I 354 (2016) 211–217

Contents lists available at ScienceDirect

C. R. Acad. Sci. Paris, Ser. I

www.sciencedirect.com

Numerical analysis

High-order accurate Lagrange-remap hydrodynamic schemes on staggered Cartesian grids

Schémas hydrodynamiques d'ordre très élevé Lagrange-projection sur grilles cartésiennes décalées

Gautier Dakin, Hervé Jourdren

CEA, DAM, DIF, 91297 Arpajon, France

ARTICLE INFO

Article history:
Received 29 July 2015
Accepted 19 November 2015
Available online 18 January 2016

Presented by the Editorial Board

ABSTRACT

We consider a class of staggered grid schemes for solving the 1D Euler equations in internal energy formulation. The proposed schemes are applicable to arbitrary equations of state and high-order accurate in both space and time on smooth flows. Adding a discretization of the kinetic energy equation, a high-order kinetic energy synchronization procedure is introduced, preserving globally total energy and enabling proper shock capturing. Extension to nD Cartesian grids is done via C-type staggering and high-order dimensional splitting. Numerical results are provided up to 8th-order accuracy.

RÉSUMÉ

Nous considérons une classe de schémas sur maillage décalé pour résoudre les équations d'Euler 1D. Les schémas proposés, formulés en énergie interne, sont d'ordre élevé en espace comme en temps, utilisables quelle que soit l'équation d'état. En ajoutant une discrétisation de l'équation de l'énergie cinétique, une procédure de synchronisation de l'énergie cinétique est introduite, préservant globalement l'énergie totale et permettant la capture correcte des chocs. Une extension nD sur grille cartésienne décalée de type C avec *splitting* directionnel d'ordre élevé est proposée. Des résultats numériques sont présentés jusqu'à l'ordre 8.

E-mail addresses: gautier.dakin.ocre@cea.fr (G. Dakin), herve.jourdren@cea.fr (H. Jourdren).

http://dx.doi.org/10.1016/j.crma.2015.11.008

1. Introduction

In the late 1940s, the first shock capturing hydrodynamic scheme by Richtmyer [9] and von Neumann and Richtmyer [14] was a staggered 1D Lagrange *explicit* scheme, formulated in internal energy with artificial viscosity and *2nd-order accuracy* in space and time on smooth flows.

In 1961, a key contribution to 1D Lagrange schemes was provided by Trulio and Trigger [12], who identified the lack of conservation of total energy with the original scheme and proposed an *implicit* conservative version, retaining spatial staggering of variables, without temporal staggering. See also Popov and Samarskii [8].

In the early 1970s, pioneered by DeBar, several multifluid Eulerian hydrocodes with interface reconstruction on 2D Cartesian grids [2,11] relied on the Trulio–Trigger *implicit* Lagrangian scheme, making use of a Lagrange-remap approach with dimensional splitting. Later, a strictly *explicit* conservative version of the Trulio–Trigger scheme was reported in [15], with a description of the so-called BBC scheme on 2D Cartesian grids, in a 1D Lagrange-remap setting with Strang dimensional splitting, and a total energy conservation result credited to Noh [7]. See also Youngs [17] for related work on nD staggered Cartesian grids.

The aim of this Note is to propose an extension path of such schemes to high-order accuracy.

We choose a finite volume approach, combining high-order Runge–Kutta time integration in the Lagrange phase, high-order 1D spatial reconstructions and remap, and as presented in [4] with Godunov-type schemes, appropriate dimensional splitting sequences.

Section 2 is devoted to the 1D Lagrange-remap staggered grid schemes and associated total energy conservation results, keys to proper shock capturing. Section 3 details the dimensional splitting procedure. Section 4 provides numerical results on standard test problems up to 8th-order accuracy.

2. High-order 1D staggered grid schemes

First, let us consider the 1D hydrodynamics system (1) closed with an arbitrary EOS such that $p = EOS(\tau, \epsilon)$ where $\rho = 1/\tau$, u, p, e, ϵ, $e_{\text{kin}} = u^2/2$ denote respectively the mass density, the velocity, the pressure and the total, internal and kinetic energies. Let us denote ρ_0 the initial mass density. Introducing the change of variable $(x,t) \rightarrow (X,t)$ satisfying $\rho \mathrm{d}x = \rho_0 \mathrm{d}X$ and using $e = \epsilon + e_{\text{kin}}$, (1) rewrites as (2) in Lagrangian coordinates:

$$\begin{cases} \partial_t \rho + \partial_x (\rho u) = 0 \\ \partial_t (\rho u) + \partial_x \left(\rho u^2 + p\right) = 0 \\ \partial_t (\rho e) + \partial_x (\rho u e + p u) = 0 \end{cases}, \tag{1}$$

$$\begin{cases} \partial_t (\rho_0 \tau) - \partial_X u = 0 \\ \partial_t (\rho_0 u) + \partial_X p = 0 \\ \partial_t (\rho_0 \epsilon) + p \partial_X u = 0 \\ \partial_t (\rho_0 e_{\text{kin}}) + u \partial_X p = 0 \end{cases}. \tag{2}$$

The principle of the Lagrange-remap approach selected here is to integrate in time the Lagrangian system (2), and then to perform a conservative remap of the variables on the initial grid. We consider a *primal* uniform Cartesian grid $\{x_{i+\frac{1}{2}}\}$ with $\Delta X = x_{i+\frac{1}{2}} - x_{i-\frac{1}{2}}$ and a *dual* grid $\{x_i\}$ with $x_i = \frac{1}{2}(x_{i+\frac{1}{2}} + x_{i-\frac{1}{2}})$. In the following, $\overline{\phi}$ and ϕ will respectively denote the space averaged value of ϕ and its point-wise value:

$$\begin{cases} \overline{\phi}_i^n = \frac{1}{\Delta X} \displaystyle\int_{x_{i-\frac{1}{2}}}^{x_{i+\frac{1}{2}}} \phi(x, t^n) \mathrm{d}x \text{ and } \phi_i^n = \phi(x_i, t^n) \text{ for } \phi \in \{\rho_0, \rho_0 \tau, \rho_0 \epsilon\} \\ \overline{\phi}_{i+\frac{1}{2}}^n = \frac{1}{\Delta X} \displaystyle\int_{x_i}^{x_{i+1}} \phi(x, t^n) \mathrm{d}x \text{ and } \phi_{i+\frac{1}{2}}^n = \phi(x_{i+\frac{1}{2}}, t^n) \text{ for } \phi \in \{\rho_0, \rho_0 u, \rho_0 e_{\text{kin}}\} \end{cases}.$$

2.1. Lagrange step

We consider Nth-order *explicit* schemes with the following notations for Runge–Kutta sequences: α_m is the time step for the mth sub-cycle, $a_{m,l}$ the m,l term of the Butcher table and θ_l the lth reconstruction coefficient for the last step. The artificial viscosity possibly applied for strong shocks [9,14,1] is denoted by q with $\Pi = p + q$.

The system (3) details one Runge–Kutta sub-cycle at time $t^{n+\alpha_m}$ and (4) details the final step at time t^{n+1}:

Table 1
Coefficients for the finite volume computation of point-wise values from cell-average ones and *vice versa*.

Order	C_0	$C_{\pm1}$	$C_{\pm2}$	$C_{\pm3}$	$C_{\pm4}$	$\widehat{C}_0$	$\widehat{C}_{\pm1}$	$\widehat{C}_{\pm2}$	$\widehat{C}_{\pm3}$	$\widehat{C}_{\pm4}$
2nd	1	0	0	0	0	1	0	0	0	0
3rd	$\frac{13}{12}$	$\frac{-1}{24}$	0	0	0	$\frac{11}{12}$	$\frac{1}{24}$	0	0	0
4th and 5th	$\frac{1067}{960}$	$\frac{-29}{480}$	$\frac{3}{640}$	0	0	$\frac{863}{960}$	$\frac{77}{1440}$	$\frac{-17}{5760}$	0	0
6th and 7th	$\frac{30251}{26880}$	$\frac{-7621}{107520}$	$\frac{159}{17920}$	$\frac{-5}{7168}$	0	$\frac{215641}{241920}$	$\frac{6361}{107520}$	$\frac{-281}{53760}$	$\frac{367}{967680}$	0
8th and 9th	$\frac{5851067}{5160960}$	$\frac{-100027}{1290240}$	$\frac{31471}{2580480}$	$\frac{-425}{258048}$	$\frac{35}{294912}$	$\frac{41208059}{46448640}$	$\frac{3629953}{58060800}$	$\frac{-801973}{116121600}$	$\frac{49879}{58060800}$	$\frac{-27859}{464486400}$

$$\begin{cases} \overline{\rho_0\tau}_i^{n+\alpha_m} = \overline{\rho_0\tau}_i^{n} + \frac{\Delta t}{\Delta X}\sum_{l=0}^{m-1} a_{m,l}\mathrm{d}u_i^{n+\alpha_l} \\ \overline{\rho_0 u}_{i+\frac{1}{2}}^{n+\alpha_m} = \overline{\rho_0 u}_{i+\frac{1}{2}}^{n} - \frac{\Delta t}{\Delta X}\sum_{l=0}^{m-1} a_{m,l}\mathrm{d}\Pi_{i+\frac{1}{2}}^{n+\alpha_l} \\ \overline{\rho_0\epsilon}_i^{n+\alpha_m} = \overline{\rho_0\epsilon}_i^{n} - \frac{\Delta t}{\Delta X}\sum_{l=0}^{m-1} a_{m,l}\overline{\Pi\delta u}_i^{n+\alpha_l} \\ x_{i+\frac{1}{2}}^{n+\alpha_m} = x_{i+\frac{1}{2}}^{n} + \Delta t\sum_{l=0}^{m-1} a_{m,l}u_{i+\frac{1}{2}}^{n+\alpha_l} \\ p_i^{n+\alpha_m} = EOS(\tau_i^{n+\alpha_m}, \epsilon_i^{n+\alpha_m}) \end{cases}, \tag{3}$$

$$\begin{cases} \overline{\rho_0\tau}_i^{n+1} = \overline{\rho_0\tau}_i^{n} + \frac{\Delta t}{\Delta X}\sum_{l=0}^{s-1} \theta_l\mathrm{d}u_i^{n+\alpha_l} \\ \overline{\rho_0 u}_{i+\frac{1}{2}}^{n+1} = \overline{\rho_0 u}_{i+\frac{1}{2}}^{n} - \frac{\Delta t}{\Delta X}\sum_{l=0}^{s-1} \theta_l\mathrm{d}\Pi_{i+\frac{1}{2}}^{n+\alpha_l} \\ \overline{\rho_0\epsilon}_i^{n+1} = \overline{\rho_0\epsilon}_i^{n} - \frac{\Delta t}{\Delta X}\sum_{l=0}^{s-1} \theta_l\overline{\Pi\delta u}_i^{n+\alpha_l} \\ \overline{\rho_0 e_{\mathrm{kin}}}_{i+\frac{1}{2}}^{n+1} = \overline{\rho_0 e_{\mathrm{kin}}}_{i+\frac{1}{2}}^{n} - \frac{\Delta t}{\Delta X}\sum_{l=0}^{s-1} \theta_l\overline{u\delta\Pi}_{i+\frac{1}{2}}^{n+\alpha_l} \\ x_{i+\frac{1}{2}}^{n+1} = x_{i+\frac{1}{2}}^{n} + \Delta t\sum_{l=0}^{s-1} \theta_l u_{i+\frac{1}{2}}^{n+\alpha_l} \\ p_i^{n+1} = EOS(\tau_i^{n+1}, \epsilon_i^{n+1}) \end{cases}, \tag{4}$$

where $\mathrm{d}\phi$ is the difference between consecutive *point-wise* values: $\mathrm{d}\phi_i = \phi_{i+\frac{1}{2}} - \phi_{i-\frac{1}{2}}$ and $\mathrm{d}\phi_{i+\frac{1}{2}} = \phi_{i+1} - \phi_i$.

To achieve high-order resolution, it is mandatory to compute the point-wise (resp. average) values from the average (resp. point-wise) ones with high-order accuracy. Table 1 gives the usual coefficients for *centered* and *symmetric* reconstructions using the first equations of (5). Although other reconstructions may be used, centered and symmetric ones are retained here and sufficient for *uniform* Cartesian grids.

$$\begin{cases} \phi_{\xi(i)} = \sum_k C_k\overline{\phi}_{\xi(i)+k} \\ \overline{\phi}_{\xi(i)} = \sum_k \widehat{C}_k\phi_{\xi(i)+k} \\ \phi_{\xi(i)} = \frac{(\rho_0\phi)_{\xi(i)}}{(\rho_0)_{\xi(i)}} \\ \delta\phi_{\xi(i)} = \sum_{k\geq 0} d_k\left(\phi_{\xi(i)+k+\frac{1}{2}} - \phi_{\xi(i)-k-\frac{1}{2}}\right) \end{cases} \quad \text{with } \xi(i) = \begin{cases} i & \text{on primal grid} \\ i+\frac{1}{2} & \text{on dual grid} \end{cases}. \tag{5}$$

The non-conservative terms $\overline{\psi\delta\phi}$ on RHS of (3) and (4) are computed by:

(i) applying the δ operator to point-wise values of ϕ using the coefficients in Table 2 and the last equation of (5);
(ii) multiplying by the point-wise value of ψ, then reconstructing average values using the right part of Table 1 and the second equation of (5).

Table 2
Coefficients for the δ operator and the interpolation of dual grid positions from primal grid ones.

Order	d_0	d_1	d_2	d_3	d_4	r_0	r_1	r_2	r_3	r_4
2nd	1	0	0	0	0	$\frac{1}{2}$	0	0	0	0
3rd	$\frac{9}{8}$	$\frac{-1}{24}$	0	0	0	$\frac{9}{16}$	$\frac{-1}{16}$	0	0	0
4th and 5th	$\frac{75}{64}$	$\frac{-25}{384}$	$\frac{3}{640}$	0	0	$\frac{75}{128}$	$\frac{-25}{256}$	$\frac{3}{256}$	0	0
6th and 7th	$\frac{1225}{1024}$	$\frac{-245}{3072}$	$\frac{49}{5120}$	$\frac{-5}{7168}$	0	$\frac{1225}{2048}$	$\frac{-245}{2048}$	$\frac{49}{2048}$	$\frac{-5}{2048}$	0
8th and 9th	$\frac{19845}{16384}$	$\frac{-735}{8192}$	$\frac{567}{40960}$	$\frac{-405}{229376}$	$\frac{35}{294912}$	$\frac{19845}{32768}$	$\frac{-2205}{16384}$	$\frac{567}{16384}$	$\frac{-405}{65536}$	$\frac{35}{65536}$

Lemma 2.1. *For all Runge–Kutta sequences, all artificial viscosities, all spatial reconstructions, the schemes (3)–(5) formulated in internal energy are conservative in mass, momentum and total energy.*

Proof. Conservation of mass and momentum is immediate, we only prove the conservation of total energy.

$$\begin{aligned}\Delta E &= \sum_i \left(\overline{\rho_0 e}_i^{n+1} - \overline{\rho_0 e}_i^{n}\right) = \sum_i \left(\overline{\rho_0 \epsilon}_i^{n+1} - \overline{\rho_0 \epsilon}_i^{n}\right) + \sum_i \left(\overline{\rho_0 e_{\text{kin}}}_{i+\frac{1}{2}}^{n+1} - \overline{\rho_0 e_{\text{kin}}}_{i+\frac{1}{2}}^{n}\right)\\ &= -\frac{\Delta t}{\Delta X}\sum_i \sum_{l=1}^{s} \theta_l \left(\overline{\Pi \delta u}_i^{n+\alpha_l} + \overline{u \delta \Pi}_{i+\frac{1}{2}}^{n+\alpha_l}\right)\\ &= -\frac{\Delta t}{\Delta X}\sum_i \sum_{l=1}^{s}\sum_k \sum_{k'} \theta_l \widehat{C}_k d_{k'} (\Pi_{i+k}^{n+\alpha_l} u_{i+k+k'+\frac{1}{2}}^{n+\alpha_l} + u_{i+k+\frac{1}{2}}^{n+\alpha_l} \Pi_{i+k+k'+1}^{n+\alpha_l}\\ &\qquad - \Pi_{i+k}^{n+\alpha_l} u_{i+k-k'-\frac{1}{2}}^{n+\alpha_l} - u_{i+k+\frac{1}{2}}^{n+\alpha_l} \Pi_{i+k-k'}^{n+\alpha_l}).\end{aligned}$$

Making the change of index $i \leftarrow i + k'$ in the first term and $i \leftarrow i + k' + 1$ in the second term of the RHS, we get the result for wall (with non-trivial definitions of ghost-cell values) or periodic boundary conditions.

$$\begin{aligned}\Delta E = -\frac{\Delta t}{\Delta X}\sum_i \sum_{l=1}^{s}\sum_k \sum_{k'} \theta_l \widehat{C}_k d_{k'} (\, &\Pi_{i+k-k'}^{n+\alpha_l} u_{i+k+\frac{1}{2}}^{n+\alpha_l} + u_{i+k-k'-\frac{1}{2}}^{n+\alpha_l} \Pi_{i+k}^{n+\alpha_l}\\ &- \Pi_{i+k}^{n+\alpha_l} u_{i+k-k'-\frac{1}{2}}^{n+\alpha_l} - u_{i+k+\frac{1}{2}}^{n+\alpha_l} \Pi_{i+k-k'}^{n+\alpha_l}) = 0. \qquad \square\end{aligned}$$

Remark 1. The lemma still holds for implicit schemes based on implicit Runge–Kutta sequences.

Remark 2. An alternative version using $\overline{\delta \Pi}$ for the momentum equation instead of $\mathrm{d}\Pi$ also preserves momentum.

2.2. Remap step

After the Lagrange step, the dual deformed grid $\{x_i^{n+1}\}$ is computed by high-order interpolation of the primal deformed grid $\{x_{i+\frac{1}{2}}^{n+1}\}$ as $x_i = \sum_{k\geq 0} r_k \left(x_{i+k+\frac{1}{2}} + x_{i-k-\frac{1}{2}}\right)$ with r_k coefficients in Table 2. All variables $(\rho\phi)$ for $\phi \in \{1, \epsilon\}$ are remapped on the primal grid $\{x_{i+\frac{1}{2}}\}$ and for $\phi \in \{1, u, e_{\text{kin}}\}$ on the dual grid $\{x_i\}$.

For the primal grid (essentially identical for the dual one), we have:

$$\overline{\rho\phi}_i^{n+1} = \frac{1}{\Delta X}\int_{x_{i-\frac{1}{2}}}^{x_{i+\frac{1}{2}}} \rho\phi(x, t^{n+1})\mathrm{d}x = \frac{1}{\Delta X}\left[\int_{x_{i-\frac{1}{2}}}^{x_{i-\frac{1}{2}}^{n+1}} \rho\phi \mathrm{d}x + \int_{x_{i-\frac{1}{2}}^{n+1}}^{x_{i+\frac{1}{2}}^{n+1}} \rho\phi \mathrm{d}x + \int_{x_{i+\frac{1}{2}}^{n+1}}^{x_{i+\frac{1}{2}}} \rho\phi \mathrm{d}x\right],$$

written in *conservative* flux-form:

$$\overline{\rho\phi}_i^{n+1} = \overline{\rho_0\phi}_i^{n+1} - \left[\frac{x_{i+\frac{1}{2}}^{n+1} - x_{i+\frac{1}{2}}}{\Delta X}(\rho\phi)_{i+\frac{1}{2}}^{*} - \frac{x_{i-\frac{1}{2}}^{n+1} - x_{i-\frac{1}{2}}}{\Delta X}(\rho\phi)_{i-\frac{1}{2}}^{*}\right]. \tag{6}$$

To compute $(\rho\phi)_{i+\frac{1}{2}}^{*}$, we use the high-order Lagrange polynomial P_{up}^{ϕ} interpolating point-wise values of $H_{\text{up}}^{\phi}(X) = \int_{-x_{\text{up}-\frac{N}{2}+\frac{1}{2}}^{n+1}}^{X} (\rho_0\phi)(y)\mathrm{d}y$ on the deformed grid, with a stencil of length $(N+1)$ leading to:

Table 3
Coefficients for the computation of staggered point-wise values from average values and *vice versa*.

Order	$Q_{\pm\frac{1}{2}}$	$Q_{\pm\frac{3}{2}}$	$Q_{\pm\frac{5}{2}}$	$Q_{\pm\frac{7}{2}}$	$Q_{\pm\frac{9}{2}}$	$\widehat{Q}_{\pm\frac{1}{2}}$	$\widehat{Q}_{\pm\frac{3}{2}}$	$\widehat{Q}_{\pm\frac{5}{2}}$	$\widehat{Q}_{\pm\frac{7}{2}}$	$\widehat{Q}_{\pm\frac{9}{2}}$
2nd	$\frac{1}{2}$	0	0	0	0	$\frac{1}{2}$	0	0	0	0
3rd	$\frac{7}{12}$	$\frac{-1}{12}$	0	0	0	$\frac{13}{24}$	$\frac{-1}{24}$	0	0	0
4th and 5th	$\frac{37}{60}$	$\frac{-2}{15}$	$\frac{1}{60}$	0	0	$\frac{401}{720}$	$\frac{-31}{480}$	$\frac{11}{1440}$	0	0
6th and 7th	$\frac{533}{840}$	$\frac{-139}{840}$	$\frac{29}{840}$	$\frac{-1}{280}$	0	$\frac{68323}{120960}$	$\frac{-353}{4480}$	$\frac{1879}{120960}$	$\frac{-191}{120960}$	0
8th and 9th	$\frac{1627}{2520}$	$\frac{-473}{2520}$	$\frac{127}{2520}$	$\frac{-23}{2520}$	$\frac{1}{1260}$	$\frac{2067169}{3628800}$	$\frac{-40111}{453600}$	$\frac{581}{25920}$	$\frac{-28939}{7257600}$	$\frac{2497}{7257600}$

$$(\rho\phi)^*_{i+\frac{1}{2}} = \frac{1}{x^{n+1}_{i+\frac{1}{2}} - x_{i+\frac{1}{2}}}\left(P^{\phi}_{\mathrm{up}}(x^{n+1}_{i+\frac{1}{2}}) - P^{\phi}_{\mathrm{up}}(x_{i+\frac{1}{2}})\right), \text{ where up} = \begin{cases} i & \text{if } x^{n+1}_{i+\frac{1}{2}} > x_{i+\frac{1}{2}} \\ i+1 & \text{otherwise} \end{cases}. \tag{7}$$

Combined with first-order upwinding, various limiters may possibly be applied on the flux $(\rho\phi)^*_{i+\frac{1}{2}}$.

2.3. Point-wise kinetic energy synchronization step

A high-order accurate synchronization is introduced on point-wise kinetic energies[1] according to (8).

(i) Compute the difference ΔK between point-wise *remapped* kinetic energy and point-wise *reconstructed* kinetic energy.
(ii) Distribute ΔK on the average values of kinetic energy and internal energy on the stencil.

$$\begin{cases} \Delta K_{i+\frac{1}{2}} = \quad \rho e_{\mathrm{kin}}{}^{n+1}_{i+\frac{1}{2}} - \frac{1}{2}\dfrac{\left((\rho u)^{n+1}_{i+\frac{1}{2}}\right)^2}{\rho^{n+1}_{i+\frac{1}{2}}} \\ \overline{\rho e_{\mathrm{kin}}}{}^{n+1}_{i+\frac{1}{2}} \leftarrow \overline{\rho e_{\mathrm{kin}}}{}^{n+1}_{i+\frac{1}{2}} - \displaystyle\sum_k \widehat{C}_k \Delta K_{i+k+\frac{1}{2}} \\ \overline{\rho\epsilon}^{n+1}_i \leftarrow \overline{\rho\epsilon}^{n+1}_i + \displaystyle\sum_k \widehat{Q}_{k+\frac{1}{2}} \Delta K_{i+k+\frac{1}{2}}. \end{cases} \tag{8}$$

Lemma 2.2. *The kinetic energy synchronization procedure is conservative in total energy.*

Proof. For periodic or wall boundary conditions, we have:

$$\Delta E = \sum_i \left(\sum_{k'} \widehat{Q}_{k'+\frac{1}{2}} \Delta K_{i+k'+\frac{1}{2}} - \sum_k \widehat{C}_k \Delta K_{i+k+\frac{1}{2}} \right) = 0. \qquad \square$$

3. High-order dimensional splitting procedure

The 1D schemes (3)–(8) are now to be used with a dimensional splitting method (DSM) on the nD system

$$\begin{cases} \partial_t \rho + \nabla.(\rho\vec{u}) = 0, \\ \partial_t(\rho\vec{\Phi}) + \nabla\cdot(\rho\vec{\Phi}\otimes\vec{u} + \vec{f}) = 0, \end{cases} \quad \text{with } \vec{\Phi} = \begin{pmatrix} \vec{u} \\ e \end{pmatrix} \text{ and } \vec{f} = \begin{pmatrix} pI_n \\ p\vec{u}^t \end{pmatrix}. \tag{9}$$

For the sake of simplicity, we only detail the 2D case. A C-type staggering is retained: variables are indexed as $\phi_{i,j}$ for $\phi \in \{\rho_0, \rho_0\tau, \rho_0\epsilon\}$, as $\phi_{i+\frac{1}{2},j}$ for $\phi \in \{\rho_0, \rho_0 u, \rho_0 e_{\mathrm{kin},u}\}$ and as $\phi_{i,j+\frac{1}{2}}$ for $\phi \in \{\rho_0, \rho_0 v, \rho_0 e_{\mathrm{kin},v}\}$.

As previous 1D schemes are based on a 1D finite volume formulation, it is mandatory to add a transverse interpolation to deduce 1D-cell-average values from 2D-cell-average ones. The procedure originates from [4]; it is extended here to staggered grids. A sweep along the x-direction proceeds as follows:

(i) interpolate along the y-direction to get 1D-cell-average values of the conservative variables according to (5) if the variable is centered along the y-direction or according to (10) if staggered (see Table 3). This way, we only get 1D-cell-average values along the x-direction, centered along the y-direction.[2]

[1] A reminiscence of DeBar's procedure first used with the 2nd-order Trulio–Trigger scheme to recover total energy conservation as kinetic energy "dissipates" during momentum remap ([17], [2] pp. 14–17). Here with higher-order accuracy, kinetic energy is updated in both Lagrange and remap steps, and point-wisely synchronized (equivalent to DeBar's procedure in the 2nd-order case).

[2] Another high-order accurate variant retains the staggering of transverse variables along the y-direction, requiring the remap of transverse variables on a third interpolated 1D grid $\{x^{n+1}_{i+\frac{1}{2},j+\frac{1}{2}}\}$ staggered along both x- and y-directions.

Table 4
Weights w_q applied on the time step for the dimensional splitting methods (DSM).

DSM Order									
	x	y	x	y	x	y	x	y	x
2nd	0.5	1.0	0.5						
3rd	0.26833009	0.91966152	−0.18799161	−0.18799161	0.91966152	0.26833009			
4th	0.5	−0.05032120	−0.27516060	0.55032120	0.55032120	0.55032120	−0.27516060	−0.05032120	0.5
5th and 6th	0.39225680	0.78451361	0.51004341	0.23557321	−0.47105338	−1.17767998	0.06875316	1.31518632	0.06875316
	−1.17767998	−0.47105338	0.23557321	0.51004341	0.78451361	0.39225680			
7th and 8th	0.31451533	0.62903065	0.99919006	1.36934946	0.15238116	−1.06458715	0.29938548	1.66335810	−0.00780559
	−1.67896928	−1.61921866	−1.55946804	−0.62383861	0.31179081	0.98539085	1.65899088	0.98539085	0.31179081
	−0.62383861	−1.55946804	−1.61921866	−1.67896928	−0.00780559	1.66335810	0.29938548	−1.06458715	0.15238116
	1.36934946	0.99919006	0.62903065	0.31451533					

(ii) Apply the 1D Lagrange scheme with extra equations for v contributions to momentum and kinetic energy ($\partial_t \rho_0 v = \partial_t \rho_0 e_{\text{kin},v} = 0$). Remap fluxes must be computed for all 1D quantities.
(iii) Reconstruct the 2D fluxes from the 1D Lagrange and remap fluxes according to (5) if the 2D variable is centered along the y-direction or according to (10) if staggered.
(iv) Apply the reconstructed 2D fluxes on 2D-cell-average values.

$$\begin{cases} \phi_{\xi(i)} = \sum_k Q_{k+\frac{1}{2}} \overline{\phi}_{\xi(i)+k+\frac{1}{2}} \\ \overline{\phi}_{\xi(i)} = \sum_k \widehat{Q}_{k+\frac{1}{2}} \phi_{\xi(i)+k+\frac{1}{2}} \end{cases} \quad \text{with } \xi(i) = \begin{cases} i & \text{on primal grid} \\ i+\frac{1}{2} & \text{on dual grid} \end{cases}. \tag{10}$$

Lemma 3.1. *The resulting nD Cartesian grid schemes are conservative in mass, momentum, and total energy.*

Proof. With the C-type staggering of variables, the nD schemes verify Lemmas 2.1 and 2.2 direction by direction and so are globally conservative in mass, momentum, and total energy for all dimensional splitting. □

Those sweeps are made according to the DSM chosen, which consists in alternatively applying the previous procedure along the x- and y-direction with appropriate weighted time steps $w_q \Delta t$ (see Table 4 based on [16]).

The high-order DSM have *negative* time steps, which are easily handled as we focus during the remap, not on the material velocity, but rather on the displacement of the Lagrangian grid.

The kinetic energy synchronization procedure is applied at each DSM time step and in each direction after remap, without altering the accuracy of the schemes.

4. Numerical results

Computations are performed with the following Runge–Kutta sequences: SSPRK3 [10] for the 2nd and 3rd orders,[3] Kutta's scheme for 4th order, the Cash–Karp scheme for the 5th order, Verner's "robust" sequences [13] for orders greater than 5. Neither artificial viscosities/hyperviscosities[4] nor limiters are used in the Lagrange and remap steps. The point-wise kinetic energy synchronization procedure is applied in all cases.

The Shu–Osher test case [10] is initialized as (11) on a $[-5:5]$ domain with a Mach 3 shock wave interacting with a sinusoidal density field. Computations till $t = 1.8$ with CFL $= 0.2$ are reported in Fig. 1(a) and highlight the robustness and high resolution of the 6th- and 9th-order schemes with only 200 cells.

The 2D vortex advection test case is used to assess the accuracy of the schemes under IEEE-754 norm for double precision. The initial condition is given by (12). Computations are performed on a $[-10:10]^2$ domain till $t = 1$ with CFL $= 0.9$, $\gamma = 1.4$ and $\beta = 5$. The L^1-errors in both space and time are computed as $\text{err}_{L^1} = \sum_n \Delta t^n \cdot \Delta x \cdot \Delta y \sum_{i,j} ||\overline{\rho\Phi}^n_{i,j} - \overline{\rho\Phi}^{\text{exact}}_{i,j}(t^n)||_{L^1}$ with $\Phi = (1, \vec{u}, \epsilon)^t$ and reported in Fig. 1(b) with excellent agreement to the expected orders.[5]

$$(\rho_0, u_0, p_0) = \begin{cases} (\frac{27}{7}, \frac{4\sqrt{35}}{9}, \frac{31}{3}) & \text{if } x \in [-5:-4[\\ (1+\frac{\sin(5x)}{5}, 0, 1) & \text{if } x \in [-4:5] \end{cases}, \tag{11}$$

[3] For stability issues, 2-stage Runge–Kutta sequences are never used.
[4] As in [4], when Cook–Cabot-type [1] LES bulk hyperviscosity is activated, numerical accuracy is limited to the 6th order.
[5] Except for the 9th-order scheme, as we limit ourselves to a Yoshida 8th-order directional splitting.

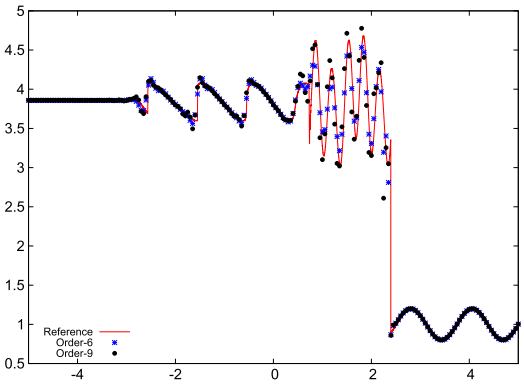

(a)

Order	EOC
2	2.014
3	2.984
4	4.013
5	4.936
6	6.052
7	6.933
8	7.996
9	8.580

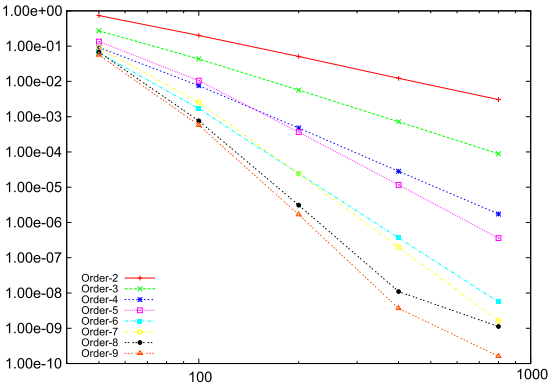

(b)

Fig. 1. (a) Shu–Osher test case on 200 cells for the 6th- and 9th-order schemes. (b) Experimental order of convergence (EOC) on the 2D advected vortex test case from the 2nd to the 9th order and L^1-error in both space and time with respect to the number of cells per direction.

$$\begin{cases} \rho_0 = \left(1 - \frac{(\gamma-1)\beta^2}{8\gamma\pi^2} e^{1-r^2}\right)^{\frac{1}{\gamma-1}} \\ \vec{u}_0 = \vec{1} + \frac{\beta}{2\pi} e^{\frac{1-r^2}{2}} \cdot (-y, x)^t \\ p_0 = \rho_0^\gamma \end{cases} . \tag{12}$$

5. Conclusion

The high-order accurate schemes proposed in this Note for solving the compressible Euler equations on C-type staggered Cartesian grids are flexible concerning (i) Runge–Kutta sequences, (ii) 1D spatial reconstructions, (iii) directional splitting methods, (iv) remap procedures, (v) artificial viscosity/hyperviscosity formulations.

Key to total energy conservation, stencils and associated coefficients used for the discretization of *non-conservative* terms in the 1D Lagrange equations for internal and kinetic energies are *centered*, *symmetric* and high-order accurate on *uniform* Cartesian grids. The proposed point-wise kinetic energy synchronization procedure enables proper *shock capturing* without altering the convergence rate for smooth flows.

Ongoing work includes integration to a hydrodynamic simulation platform [6] for comparison with Godunov-type schemes [5,4], especially on problems where high-order accuracy is valuable as long-range aeroacoustic propagation [3], vortex dynamics and LES subgrid-scale modeling.

References

[1] A.W. Cook, W.H. Cabot, Hyperviscosity for shock-turbulence interactions, J. Comput. Phys. 203 (2005) 379–385.
[2] R.B. DeBar, Fundamentals of the KRAKEN code, Lawrence Livermore Laboratory Report, Technical Report UCIR-760, 1974.
[3] S. Del Pino, B. Després, P. Havé, H. Jourdren, P.F. Piserchia, 3D finite volume simulation of acoustic waves in the Earth atmosphere, Comput. Fluids 38 (4) (2009) 765–777.
[4] F. Duboc, C. Enaux, S. Jaouen, H. Jourdren, M. Wolff, High-order dimensionally split Lagrange-remap schemes for compressible hydrodynamics, C. R. Acad. Sci. Paris, Ser. I 348 (2010) 105–110.
[5] O. Heuzé, S. Jaouen, H. Jourdren, Dissipative issue of high-order shock capturing schemes with non-convex equations of state, J. Comput. Phys. 228 (2009) 833–860.
[6] H. Jourdren, HERA: a Hydrodynamic AMR Platform for Multi-Physics Simulations, LNCSE, vol. 41, Springer, 2005, pp. 283–294.
[7] W.F. Noh, Numerical methods in hydrodynamic calculations, Lawrence Livermore Laboratory Report, Technical Report UCRL-52112, 1976.
[8] Y.P. Popov, A.A. Samarskii, Completely conservative difference schemes, Zh. Vychisl. Mat. Mat. Fiz. 9 (4) (1969) 953–958.
[9] R.D. Richtmyer, Proposed numerical method for calculation of shocks, Los Alamos Report, 671, 1948.
[10] C.-W. Shu, S. Osher, Efficient implementation of essentially non-oscillatory shock-capturing schemes, II, J. Comput. Phys. 83 (1989) 32–78.
[11] W.G. Sutcliffe, BBC hydrodynamics, Lawrence Livermore Laboratory Report, Technical Report UCID-17013, 1974.
[12] J.G. Trulio, K.R. Trigger, Numerical solution of the one dimensional Lagrangian hydrodynamics equations, Lawrence Radiation Laboratory Report, Technical Report UCRL-6267, 1961.
[13] J.H. Verner, Jim Verner's Refuge for Runge–Kutta pairs, http://people.math.sfu.ca/~jverner/, 2013.
[14] J. von Neumann, R.D. Richtmyer, A method for numerical calculation of hydrodynamic shocks, J. Appl. Phys. 21 (1950) 232–237.
[15] P. Woodward, P. Colella, The numerical simulation of two-dimensional fluid flow with strong shocks, J. Comput. Phys. 54 (1984) 115–173.
[16] H. Yoshida, Construction of higher order symplectic integrators, Phys. Lett. A 150 (1990) 262–267.
[17] D.L. Youngs, The Lagrangian remap method, in: Implicit Large Eddy Simulation: Computing Turbulent Flow Dynamics, Cambridge University Press, Cambridge, UK, 2007.